Developmental Biology 321 (2008) 101–110

Contents lists available at ScienceDirect

Developmental Biology

journal homepage: www.elsevier.com/developmentalbiology

barx1 is necessary for ectomesenchyme proliferation and osteochondroprogenitor condensation in the zebrafish pharyngeal arches

Steven M. Sperber *, Igor B. Dawid

Laboratory of Molecular Genetics, Eunice Kennedy Shriver National Institute of Child Health and Human Development, 9000 Rockville Pike, Bethesda, MD 20892, USA

ARTICLE INFO

Article history:
Received for publication 18 October 2007
Revised 2 June 2008
Accepted 3 June 2008
Available online 13 June 2008

Keywords:
Barx1
Pharyngogenesis
Viscerocranium
Zebrafish
Pharyngeal arches
Neural crest
Chondrogenesis
Cartilage
BMP
FGF

ABSTRACT

Barx1 modulates cellular adhesion molecule expression and participates in specification of tooth-types, but little is understood of its role in patterning the pharyngeal arches. We examined *barx1* expression during zebrafish craniofacial development and performed a functional analysis using antisense morpholino oligonucleotides. *Barx1* is expressed in the rhombencephalic neural crest, the pharyngeal arches, the pectoral fin buds and the gut in contrast to its paralogue *barx2*, which is most prominently expressed in the arch epithelium. Additionally, *barx1* transient expression was observed in the posterior lateral line ganglia and developing trunk/tail. We show that Barx1 is necessary for proliferation of the arch osteochondrogenic progenitors, and that morphants exhibit diminished and dysmorphic arch cartilage elements due to reductions in chondrocyte differentiation and condensation. Attenuation of Barx1 results in lost arch expression of osteochondrogenic markers *col2a1*, *runx2a* and *chondromodulin*, as well as odontogenic marker *dlx2b*. Further, loss of *barx1* positively influenced *gdf5* and *chordin*, markers of jaw joint patterning. FGF signaling is required for maintaining *barx1* expression, and that ectopic BMP4 induces expression of *barx1* in the intermediate region of the second pharyngeal arch. Together, these results indicate an essential role for *barx1* at early stages of chondrogenesis within the developing zebrafish viscerocranium.

Published by Elsevier Inc.

Introduction

The viscerocranium consists of highly adapted skeletal elements derived from the embryonic pharyngeal arch ectomesenchyme that function in concert but allow for diverse pharyngolaryngeal activities. The viscerocranium is composed of membranous and endochondral bones. Endochondral bone formation within the pharyngeal arches is a multi-step process that requires the migration of the cranial neural crest into the facial prominences and their subsequent epitheliomesenchymal interactions; these interactions are necessary for fate determination, aggregation of the cells into discrete condensations, and their terminal differentiation (Hall and Miyake, 2000; Helms and Schneider, 2003; Goldring et al., 2006). Signaling factors that include Bone Morphogenic Proteins (BMPs) and Fibroblast Growth Factors (FGFs), through reciprocal epitheliomesenchymal interactions, influence the expression of downstream factors that pattern the chondrogenic elements (de Crombrugghe et al., 2000; Hall and Miyake, 2000; Tuan, 2004; Goldring et al., 2006). The precise mechanism of patterning osteochondrogenic progenitors is not well understood.

The Barx family of homeodomain-containing transcription factors participates in the formation of mesenchymal condensations through the modulation of cellular adhesion molecules (CAMs), and regulation of fibril-forming type II collagen (*Col2a1*) (Jones et al., 1997; Edelman et al., 2000; Meech et al., 2005). The regulation of CAMs and *Col2a1*, a major component of the cartilage extracellular matrix, by *Barx1* indicates a direct link between expression of a tissue-specific transcription factor and changes in cartilage morphology. In the mouse, *Barx1* expression is located at sites of mesenchymal condensation that include the pharyngeal arches, the limb buds, developing joints, molar tooth papillae and the stomach wall (Tissier-Seta et al., 1995; Jones et al., 1997; Barlow et al., 1999; Kim et al., 2005). Ectopic *Barx1* gene expression in mouse mandible cultures results in the alteration of incisor teeth to an unusual molariform shape (Tucker et al., 1998; Miletich et al., 2005), while attenuation of *Barx1* by RNA interference results in arrest of molar mesenchyme at the bud stage (Song et al., 2006). Manipulation of the closely related *Barx2* gene expression in limb bud cultures affects cellular aggregation and chondrocyte differentiation, indicating a familial role in patterning chondrocytes (Meech et al., 2005). The function of *Barx1* in craniofacial development has yet to be fully examined. In humans, rare duplications and deletions of the BARX1 locus result in craniofacial and joint anomalies, but no disease-causing mutations have been associated directly with this gene (Stalker et al., 1993; Gould and Walter, 2000;

* Corresponding author. Building 6B, Room 422, 9000 Rockville Pike, National Institutes of Child Health, Bethesda, MD 20892, USA. Fax: +1 301 496 0243.
E-mail address: sperbers@mail.nih.gov (S.M. Sperber).

0012-1606/$ – see front matter. Published by Elsevier Inc.
doi:10.1016/j.ydbio.2008.06.004

Gould and Walter, 2004; Redon et al., 2006). To explore the relationship of this gene with craniofacial development we characterized zebrafish *barx1* and the phenotype on the *barx1* morphant.

Here we show that the zebrafish *barx1* gene is expressed in the migrating cranial neural crest and subsequently in the developing cartilage elements of the pharyngeal arches. Transient expression is observed in the posterior lateral line ganglia and in the trunk and tail. In contrast to *barx1*, the *barx2* paralogue is expressed predominantly in the proximal aspects of the fin buds and in oral and aboral epithelium of the first and second pharyngeal arches. Attenuation of *barx1* expression using antisense morpholinos results in a loss of arch cartilage tissue and micrognathia without an increase in apoptosis, but with a reduction in Phosphohistone-H3 stained nuclei, indicating a role for *barx1* in cellular proliferation and chondrocyte differentiation. As FGF and BMP signaling are known to pattern arch development, we examined the influence of these factors on *barx1* expression. Examination of mutant embryos deficient in *fgf3* (*lia*) and *fgf8* (*ace*), as well as embryos treated with an FGF receptor antagonist (SU5402), show that FGF signaling is necessary for maintaining and patterning *barx1* expression in the arches. In contrast, ectopic BMP4 signaling induces misspecification of *barx1* patterning within the intermediate aspect of the second pharyngeal arch. This work provides insight into *barx1* function and patterning during prechondrogenic condensation events in the developing zebrafish viscerocranium.

Materials and methods

Animal maintenance and transgenic zebrafish

Zebrafish embryo lines, EK wild-type, *fli1:GFP* transgenics (Motoike et al., 2000), and the *fgf8/ace* mutant, were maintained according to Westerfield (1995). Fixed wild-type and sibling *fgf3/lia* embryos were a gift from the Hammerschmidt laboratory (Germany). Embryos and larvae were fixed in 4% paraformaldehyde/phosphate buffered saline and dehydrated in methanol for storage at −20 °C. FGF inhibition was performed by soaking 24 hour post-fertilization (hpf) embryos in 10 μm SU5402 (Pfizer) in 5% DMSO.

In vitro transcription of synthetic RNA

The zebrafish *barx1* (NM001024949) and the *barx2* predicted open reading frame (XM001342008) were amplified from cDNA produced by reverse transcription from 96 hpf RNA and cloned into pCRII-TOPO (Invitrogen). For capped sense mRNA, the *barx1* open reading frame was cloned into pCS2+ plasmid, digested with Not I, and transcribed with SP6 Polymerase. Capping was performed with 7′ methylguanosine GTP analogue cap (NEB).

Attenuation of barx1 expression

Morpholinos (MO) complementary to the translational start site of *barx1* (*Bx MO*) and the splice acceptor (*Sa MO*) of the second exon (Fig. 1A) were microinjected into one to two cell-stage embryos. Lissamine conjugated MOs (Gene-Tools) used are as follows: *Bx MO*, [5′ CCCCAATCTCCAAAGGATGTTGCAT3′], *Sa MO* [5′GCCTTCAGAACTGGAATG AAATAAG3′], and a standard control [5′CCTCTTACCTCAGTTA-CAATTTATA3′]. MOs were diluted in Danieau buffer (58 mM NaCl, 0.7 mM KCl, 0.4 mM $MgSO_4$, 0.6 mM $Ca(NO_3)_2$, 5 mM Hepes, pH 7.6) and 0.01% Phenol Red. Embryos were injected with approximately 1 nl of MO at a concentration of 4 ng/nl. For rescue, the MOs were co-injected with 25 ng/μl of *barx1* mRNA containing five base pair mismatches within the ATG MO target site. To test inhibition of translation, a *barx1:eGFP* fusion construct was injected together with the MO, and proteins extracted from 24 hpf embryos were blotted with anti-*gfp* (1/1000; Santa Cruz) and anti-α-*tubulin* (1/1000; CalBiochem) antibodies, and detected by a Dura Chemiluminescence Kit (Pierce). To test the effectiveness of the Sa MO, total RNA was extracted from 24 hpf morphant and control embryos, DNase I treated and column purified (Qiagen). RT-PCR, using random hexamer primers was performed on 1 μg of RNA for each sample (Superscript III, Invitrogen). Forward (5′-AATGCAACATCCTTTGGAGATT-3′) and reverse (5′-ATCCCGTTTATTCCTCTTGGTT-3′) primers were used to test for properly spliced *barx1* mRNA. β-*actin* amplification was used as a control.

Whole-mount in situ hybridization and histological characterization

The following antisense riboprobes were used: *chondromodulin* (AF322374) (Sachdev et al., 2001); *col2a1* (U23822) (Yan et al., 1995); *crestin* (AF195881) (Luo et al., 2001); *dlx2a* (NM131311) (Akimenko et al., 1994); *dlx2b* (NM131297) (Jackman et al., 2004); *crestin* (Rubinstein et al., 2000; Luo et al., 2001); *goosecoid* (*gsc*) (NM131017) (Stachel et

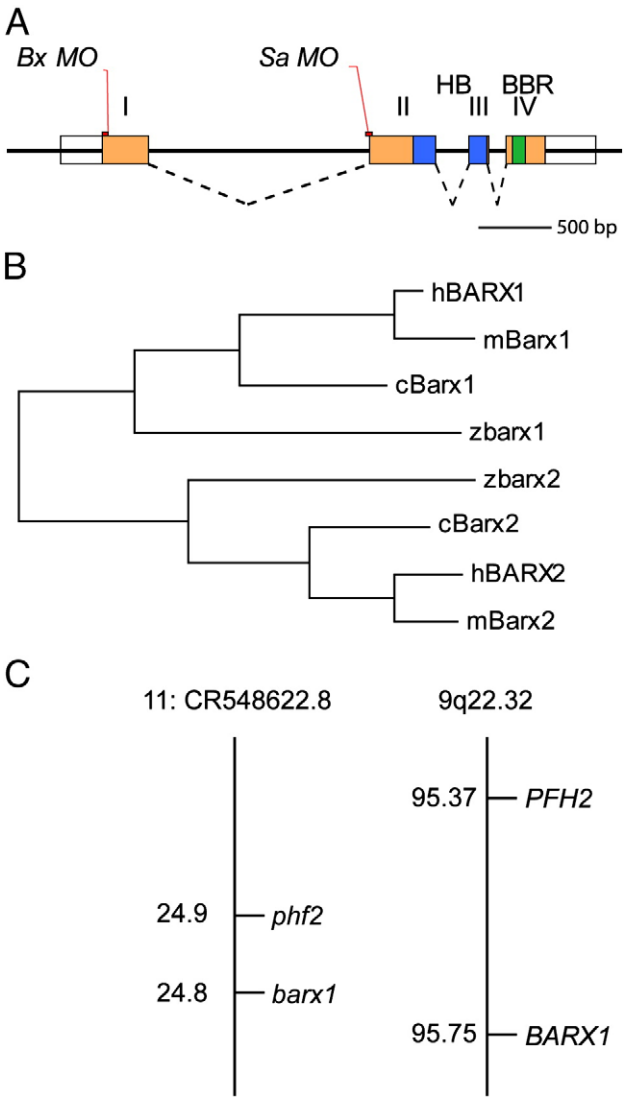

Fig. 1. Molecular analysis of zebrafish *barx1*. (A) The coding region of *barx1* consists of four exons (boxes, numbered with Roman numerals) containing the homeobox (HB, blue) and the Bar Basic Region (BBR, green); UTR's are indicated by outlined boxes. Target sites of the *barx1* ATG morpholino (*Bx MO*) and the splice-acceptor site morpholino (*Sa MO*) are indicated. (B) Phylogenetic tree comparing zebrafish (z) Barx1 with the human (h), mouse (m), and chicken (c) Barx amino acid sequences, as examined using ClustalW. GenBank accession nos.: (h1) NM021570, (m1) NM007526, (c1) NM204193, (z1) NM001024949, (h2) NM003658, (m2) NM013800, (c2) NM204896, (z2) XM001342008 respectively. (C) Syntenic relationship between zebrafish chromosome 11 fragment contig: CR548622.8 (Ensembl release 49, March 2008) and the human chromosome 9q22.32 (loci distances indicated in Mb). The *barx1* and *phf2*, PHD finger protein 2, are linked in zebrafish and humans.

al., 1993); *hand2* (*dhand*; NM131626) (Angelo et al., 2000); *inca* (Luo et al., 2007); *neurod*, (NM130978) (Korzh et al., 1998); *runx2b* (NM212862) (Flores et al., 2004); and *sox9a* (NM161343) (Chiang et al., 2001). Whole-mount *in situ* hybridizations were performed as described by Akimenko et al. (1994), using anti-digoxigenin, and anti-fluorescein antibodies (Roche).

Phosphohistone-H3 antibody (Upstate) was used at 1/1000 dilution, followed by anti-mouse biotinylated secondary antibody (Vectastain). Cartilage staining was performed as in Ellies et al., (1997). Histological analysis was performed on embryos embedded in JB-4 plastic (Polysciences) and serially sectioned. Sections were stained with 13% Methylene blue and 0.13% Basic Fuchsin. Apoptosis was determined by TUNEL labeling, using Terminal Transferase (Roche) and dUTP-DIG (Roche) as described in Ellies et al. (1997).

Bead implantation

Recombinant BMP4 (1 μg/ml) (R and D Systems) was used with Affi-Gel Blue beads (Bio-Rad). One percent BSA coated Heparin beads (Sigma) were used as control. Beads were soaked at 4 °C overnight. A sharp needle (Fine Instruments) was used to embed beads anterior to the otic vesicle on the left side of the embryo.

Photography

Samples were digitally photographed with a Leica MZ APO dissecting microscope connected to a computer running Northern Eclipse 6.0 image capture software (Empix Imaging Inc.). Live animals were immobilized with tricaine and mounted in egg water or methylcellulose. For higher magnification, fixed embryos were cleared in glycerol and digitally photographed using a Zeiss Axioplan 2.

Results

Zebrafish barx1 is the orthologue of the mouse and human Barx1 genes

The sequence encoding zebrafish *barx1* has recently been deposited in GenBank (accession no. NM001024949). Vertebrates have at least two *barx* genes, and BLAST-searches of the most recent version of the zebrafish genome (Zv7), yielded two *barx* paralogues, *barx1* and a predicted *barx2* (XM001342008) located on chromosome 17. The *barx1* open reading frame is encoded in four exons and includes an engrailed homology (EH) domain, the homeobox (HB) and a conserved Bar Basic Region (BBR, Fig. 1A, Supplementary Fig. S1). The Bar Basic Region is thought to assist in both positive and negative regulation of downstream genes in a tissue-specific manner (Edelman et al., 2000). Similarly, the *barx2* sequence indicates a conservation of the EH, HB and BBR domains. ClustalW alignment and phylogenetic analysis of the zebrafish, human, mouse and chick Barx proteins indicate that the zebrafish *barx1* gene is closely related to the *Barx1* clade (Fig. 1B; Supplementary Fig. S1). The zebrafish *barx1* gene, located on chromosome 11 (DNA contig: CR548622.8; Zv7 genome assembly; Ensembl release 49, March 2008), exhibits conserved synteny with human *BARX1* located on chromosome 9q22.32 (Ensembl release 49), but not with human *BARX2* located on chromosome 11q24.3 (Hjalt and Murray, 1999), confirming orthology between the two genes (Fig. 1C).

barx1 expression in the developing zebrafish embryo

In zebrafish, *barx1* expression has been previously described and used as a marker of patterning within the developing pharyngeal arches (Walker et al., 2006; Walker et al., 2007); however, its expression pattern has not been fully characterized. To further understand its role in development, we performed a series of *in situ* hybridizations in embryos from the one-cell stage to 120 hour post-fertilization (hpf) larvae. Transcripts of *barx1* were not detected by RT-PCR or whole-mount *in situ* hybridization prior to somitogenesis (data not shown). We observed expression at 9 somites (13 hpf) during the initiation of rhombencephalic neural crest migration in bilateral domains on either side of the neural tube (arrows; Figs. 2A, B). Cells expressing *barx1* appear to be a subset of the rhombencephalic neural crest, as these cells are located in the most ventral aspect of the streams compared to the pan-neural crest marker *crestin* (*ctn*, red) (Figs. 2C, D). At 24 hpf, expression was observed in the three streams of the cranial neural crest, in the gut primordia, fin

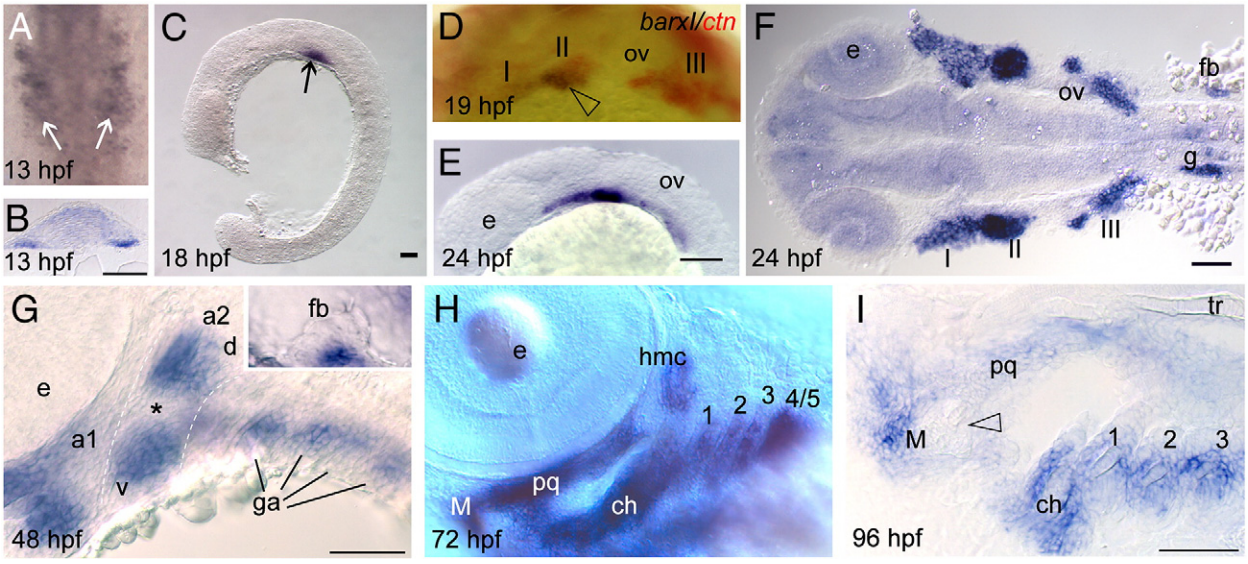

Fig. 2. *Barx1* expression. Embryos at (A, B) 13 hpf, (C)18 hpf, (D) 19 hpf, (E, F) 24 hpf, (G) 48 hpf, (H) 72 hpf, and (I) 96 hpf, were examined by *in situ* hybridization. (A) *barx1* expression in the migrating neural crest in bilateral domains adjacent to the hindbrain (arrows). Anterior is at the top. (B) Coronal section through the hindbrain. (C) Lateral view of *barx1* expression (arrow). (D) Double *in situ* of *barx1* (dark blue, arrowhead) and *crestin* (red) co-expression in the neural crest streams indicated by Roman numerals. (E, F) Expression in the cranial neural crest streams. (G, G inset) *barx1* expression in the pharyngeal arches and fin bud; a1, first arch; a2, second arch; d, dorsal expression domain; ga, gill arches; v, ventral expression domain; asterisk indicates the a2 intermediate region. (H) Lateral oblique view of *barx1* expression in the chondrocytes. (I) Parasagittal section, open arrowhead indicates jaw joint. ch, ceratohyal; ceratobranchials are numbered; e, eye; fb, fin bud; g, gut primordium; hmc, hyomandibular condensation; M, Meckel's cartilage; ov, otic vesicle; pq, palatoquadrate; tr, trabecula. Scale bar: (B and I) 50 μm; (C, E–G) 100 μm.

bud primordia and in the trunk and tail (Figs. 2E, F; Supplementary Figs. S2A, B). Trunk and tail expression was progressively lost by 48 hpf (Supplementary Figs. S2A–C). Transcripts in the differentiating ectomesenchyme of the pharyngeal arches at 48 hpf were concentrated in the developing prechondrogenic condensations (Fig. 2G). *Barx1* expression within the dorsal aspect of the second arch appeared to be rostrally enriched, potentially correlating with sites of increased proliferation within the hyomandibular condensation that subsequently fuses with the symplectic element (Kimmel et al., 1998). Expression was also maintained in the pectoral fin bud (Fig. 2G, inset). In mammals, Barx1 participates in tooth development (Tucker et al., 1998; Song et al., 2006; Mitsiadis and Drouin, 2008). We examined whether *barx1* is expressed in the developing tooth buds at 56 hpf, a time when tooth primordia are readily observable (Jackman et al., 2004) (asterisk, Supplementary Fig. S2D). Expression of *barx1* appears to be adjacent to the condensing tooth bud primordia. In 72 hpf embryos, *barx1* continued to be expressed for the most part in the stacked arrays of chondrogenic cells, but diminishes as the elements mature (Fig. 2H and data not shown). At this time, we also identified *barx1* expression in the posterior lateral line ganglia (pllg, Supplementary Figs. S2E, F, H, H inset). Transcripts of *barx1* continued to be detected in the intestinal wall of the gut (Supplementary Figs. S2H, I). By 96 hpf, serial sections of larvae showed a progressive loss of *barx1* expression in the stacked

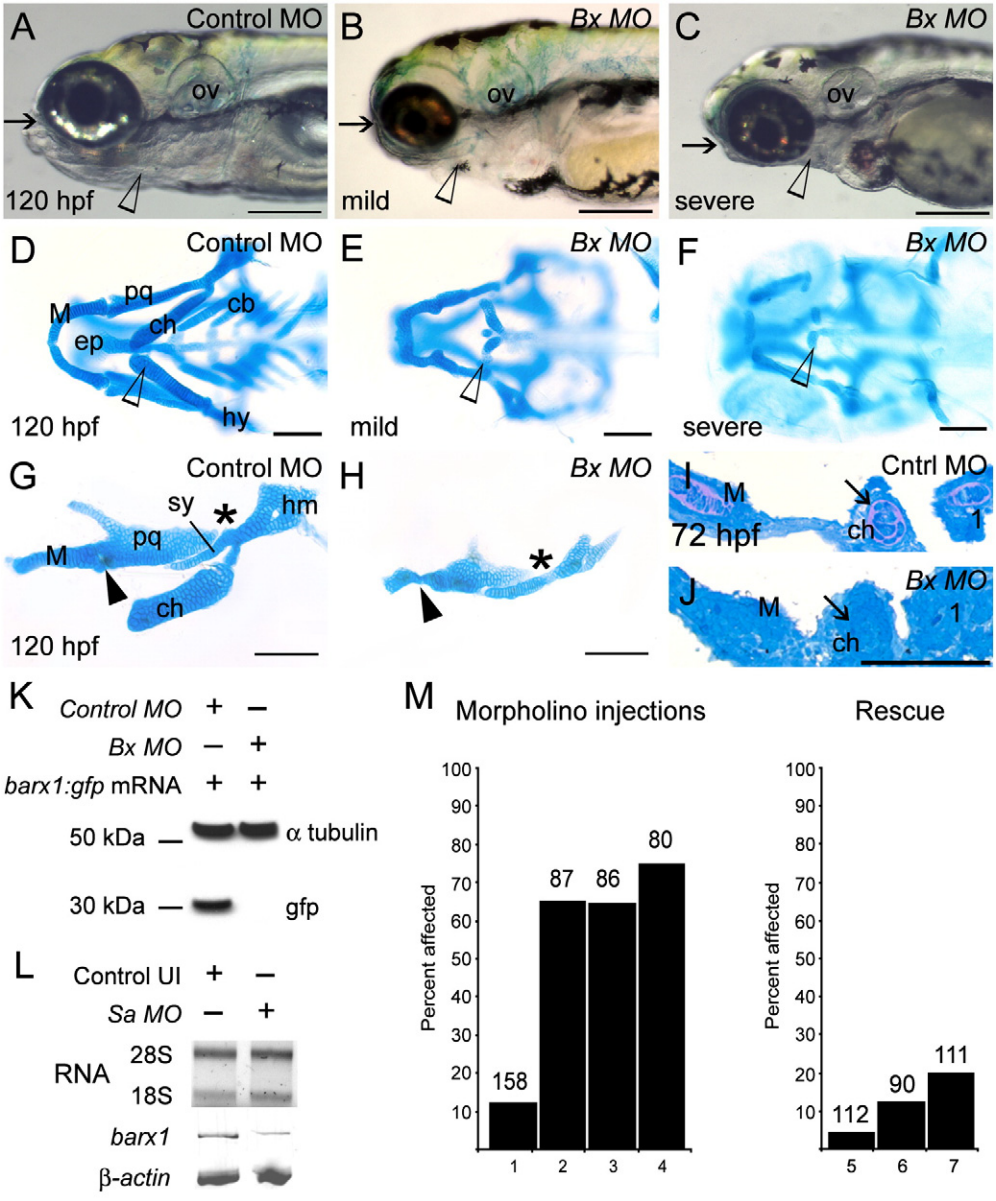

Fig. 3. Attenuation of *barx1* expression perturbs viscerocranial morphology and cartilage patterning. Larvae injected with (A) control MO (4 ng), and (B and C) *Bx MO* (4 ng). Alcian Blue staining of control MO (D) and *Bx MO* injected (E and F) 120 hpf larvae. Dissection of the first and second arches of control (G) and mildly affected larvae (H). (I and J) Parasagittal sections of 72 hpf embryos. (J) *Bx MO* (4 ng) injected compared with (I) control MO injected (4 ng). Anterior is to the left; (A–C, G–J) lateral views, (D–F) ventral view. (A–C) Arrows indicate mouth, and arrowheads the pharyngeal arches; (D–F) open arrowheads indicate the ceratohyal cartilage; (G, H) asterisk, perturbed fusion; black arrowhead, joint fusion between Meckel's cartilage (M) and the palatoquadrate (pq); cb, ceratobranchials; ch, ceratohyal; ep, ethmoid plate; hm, hyomandibular; ov, otic vesicle; sy, symplectic element. Scale bars: (A–C) 250 μm; (D–H) 100 μm; (J) 50 μm. (K, L) Effectiveness and specificity of the *barx1* (Bx) and splice-acceptor (Sa) morpholinos. (K) Western analysis of *in vivo* attenuation of *barx1:GFP* translation in 24 hpf zebrafish embryos. (L) Total RNA extracts (18S and 28S bands shown) used for RT-PCR of *barx1*. β-*actin* used as a control. (M) Percentage of affected embryos comparing control MO, *Bx MO* and *Sa MO*, and rescue by co-injection of *barx1* mRNA with a 5-bp mismatch to the ATG target site. Affected embryos are defined as those exhibiting micrognathia as a result of a reduction or loss of arch cartilage elements, as seen by Alcian Blue staining at 120 hpf. (1) Control MO 4 ng; (2) *Bx MO* 4 ng; (3) *Sa MO* 4 ng; (4) *Bx MO* 2 ng+*Sa MO* 2 ng. Rescue: (5) *gfp* mRNA 25 pg; (6) *barx1* mRNA 25 pg; (7) *Bx MO*+*Sa MO* 2 ng each+*barx1* mRNA 25 pg. Number of embryos indicated on top of each bar.

cartilage cells, with expression remaining in the surrounding mesenchyme (Fig. 2I). In summary, expression in the head skeleton was restricted to the ectomesenchyme of the developing pharyngeal arches up to 120 hpf, and was not observed in the neurocranium.

To determine whether there might be genetic redundancy between *barx1* and *barx2*, we examined the expression pattern of the *barx2* paralogue (Supplementary Fig. S3). In contrast to *barx1*, *barx2* is expressed in the proximal aspect of the pectoral fin buds from 24 to 32 hpf (Supplementary Figs. S3A–C). From 36 hpf to 72 hpf, expression is observed in the oral and aboral epithelium of the mandibular and hyoid arches (Supplementary Figs. S3D–H), and not in the condensing mesenchyme of the chondrogenic elements (arrowheads, Supplementary Fig. S3G). Expression is also observed in the olfactory epithelium (Supplementary Fig. S3F inset). The expression patterns of *barx1* and *barx2* do not overlap in the condensing mesenchyme of the prechondrogenic elements, suggesting that limited or no genetic redundancy exists between the paralogues.

barx1 is necessary for pharyngeal arch chondrogenesis

To determine the role of *barx1* in the developing pharyngeal arches and viscerocranium, we used antisense morpholinos (MO) targeted to the ATG site (*Bx MO*) and a splice-acceptor site (*Sa MO*) (Fig. 1A). MOs were injected into 1–2 cell embryos, and development was followed to 120 hpf. Compared to control MO-injected larvae at 120 hpf, morphants exhibited reduction in head size ranging from mild to severe hypoplastic pharyngeal arch morphology exemplified by micro- or agnathia (Figs. 3A–C, arrow), due to poor pharyngeal arch outgrowth (open arrowhead, Figs. 3A–C). Alcian Blue staining showed reductions or a lack of pharyngeal arch-derived chondrogenic elements (Figs. 3D–F). Generally, all the elements were dysmorphic, while the ceratobranchial elements were the most likely to be lost, which included the fifth arch elements containing the pharyngeal teeth. The most severely affected larvae exhibited either small cartilage nodules in place of elements or lacked any cartilage in the viscerocranium (open arrowhead, Fig. 3F, and data not shown). In more mildly affected larvae, reductions in chondrocyte condensation and incomplete fusions were observed between the symplectic and the hyomandibular elements (asterisk, Figs. 3G, H), as well as abnormal joint fusions between Meckel's cartilage and the palatoquadrate element (black arrowhead, Figs. 3G, H). Histological examination of larvae at 72 hpf during cartilage condensation in the pharyngeal arches showed a lack of cellular organization within the arches, as shown by a deficiency of prechondrocyte aggregation and absence of characteristic extracellular matrix surrounding the cells (arrow, Figs. 3I, J; see also boxed region in Supplementary Figs. S4A, B).

To test the effectiveness of the *Bx MO*, a *barx1:GFP* fusion mRNA containing the ATG MO target site was co-injected with the morpholino into 1–2 cell embryos. Western blot analysis at 24 hpf showed that the morpholino effectively inhibited *barx1:GFP* translation indicating that injected embryos are strong hypomorphs (Fig. 3K). Additionally, to verify that the phenotype was due to the attenuation of *barx1* translation, the second MO targeting the second exon splice-acceptor site was tested (*Sa MO*; Fig. 1A). RT-PCR of Sa MO-injected embryo RNA extracts showed a reduced amount of product of spliced mRNAs when compared to control embryos (Fig. 3L). Embryos injected with 4 ng of *Bx MO* or the *Sa MO* exhibited identical phenotypes of dysmorphic viscerocranial patterning at similar frequencies (Fig. 3M, bars 2 and 3). Co-injection of both *Bx MO* and *Sa MO* (2 ng each) produced the same phenotype with a higher effectiveness (Fig. 3M, bar 4). Finally, rescue of the phenotype was achieved by co-injecting both morpholinos with *barx1* mRNA containing a 5-base pair mismatch in the ATG target sequence (Fig. 3M, bar 7). Injection of 25 pg mRNA, used for rescue, was not deleterious, but higher doses (50 pg) of mRNA caused most embryos to exhibit aberrant gastrulation.

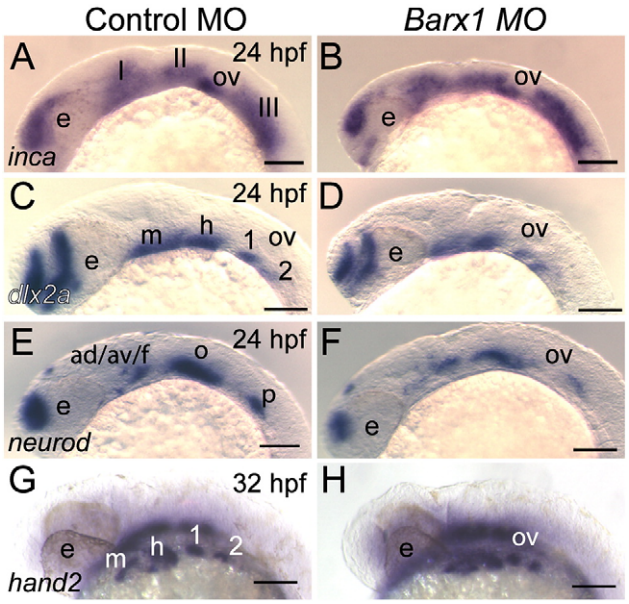

Fig. 4. Initial patterning of the arches is maintained in *barx1* morphants. (A, C, E and G) Control MO-injected embryos, (B, D, F and H) embryos co-injected with *Bx MO*+*Sa MO*, 2 ng each. Neural crest expression of *inca* (A, B) and *dlx2a* (C and D) at 24 hpf. (E, F) *neurod* expression at 24 hpf in neural ganglia precursors; (G and H) *hand2* expression in ventral endoderm at 32 hpf. Neural crest streams marked in Roman numerals, gill arches indicated by numbers; e, eye; m, mandibular arch; h, hyoid arch; ov, otic vesicle; ad/av/f, anterodorsal/anteroventral lateral line/facial placode/ganglia; o, octavel/statoacoustic ganglia precursors; p, posterior lateral line placode/ganglion. Scale bar: 100 μm.

barx1 is not required for early neural crest specification

To test whether *barx1* participates in specification of the prechondrocyte lineage, we examined cranial neural crest markers expressed in the migrating cells in *barx1* morphants. Molecular markers of the cranial neural crest (see Materials and methods) that include *inca* (Figs. 4A, B), *dlx2a* (Figs. 4C, D), as well as *neurod*, a marker of nascent ganglion cells (Figs. 4E, F), and *hand2*, an endodermal marker, were tested (Figs. 4G, H). In all cases, expression patterns of these markers in *barx1* morpholino-injected embryos appeared normal at 24 hpf, although development of the injected embryos appeared mildly delayed. This suggests that a deficiency in *barx1* expression does not strongly affect specification and migration of the hindbrain-derived neural crest. Likewise, examination of *fli1:GFP barx1* morpholino-injected embryos that express GFP in the pharyngeal arches (Lawson and Weinstein, 2002; Crump et al., 2004), suggested that neural crest migration into the arches is normal (Supplementary Figs. S4C–F).

Pharyngeal arch chondrocyte differentiation requires barx1

To determine the role of *barx1* in cartilage patterning, we examined markers of differentiation of osteochondroprogenitor cells in MO-injected embryos. The expression patterns examined included *goosecoid* (*gsc*), a marker of cellular condensation in the hyoid arch (Schulte-Merker et al., 1994); *sox9a*, a transcription factor necessary for chondrogenesis (Yan et al., 2002; Yan et al., 2005); *runx2b*, a marker of mesenchymal condensations and chondrocyte differentiation (Flores et al., 2006); fibril-forming *type II collagen* (*col2a1*), the major component of the cartilage extracellular matrix (Yan et al., 1995), *chondromodulin* (*chm*), a secreted glycoprotein that stimulates maturation of chondrocytes and inhibits vascularization (Sachdev et al., 2001); and *dlx2b*, a marker of tooth differentiation on the fifth ceratobranchial arch (Jackman et al., 2004) (Fig. 5). While the heads of *barx1* morphants were reduced in size compared to controls, *gsc* and *sox9a* expression

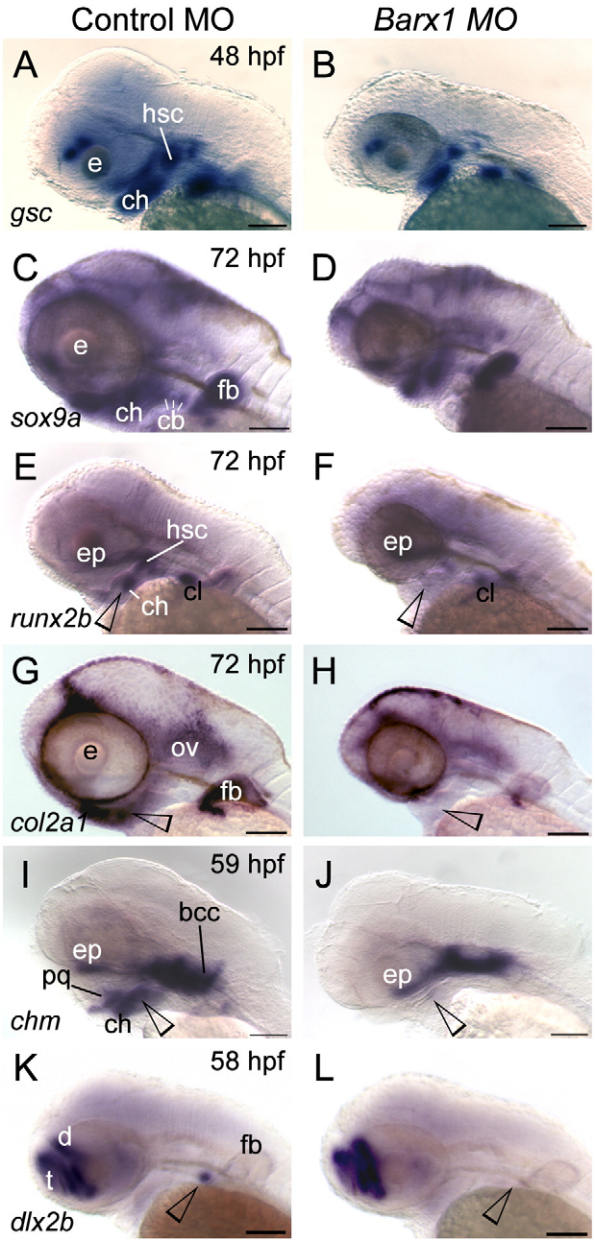

Fig. 5. *Barx1* is necessary for expression of chondrogenic markers within the pharyngeal arches. (A, C, E, G, I and K) Control embryos; (B, D, F, H, J and L) *barx1* morphant embryos (see Fig. 4). Whole-mount *in situ* hybridization for (A, B) *goosecoid* (*gsc*), (C, D) *sox9a*, (E, F) *runx2b*, (G, H) *type II collagen* (*col2a1*), (I, J) *chondromodulin* (*chm*), and (K, L) *dlx2b*. Anterior is to the left; open arrowheads indicate sites of altered marker expression in the morphants; bcc, basicranial commissures; cb, ceratobranchials; ch, ceratohyal; cl, cleithrum; d, diencephalon; ep, ethmoid plate; fb, fin bud; hsc, hyosymplectic condensation; ov, otic vesicle; pq, palatoquadrate; t, telencephalon. Scale bar: 100 μm.

was maintained in the hypoplastic arches, suggesting that *gsc* and *sox9a* expression may be regulated independently of *barx1* (Figs. 5A–D). However, molecular markers of the chondrogenic and subsequent osteogenic program, *col2a1*, *chm*, and *runx2b*, were reduced or lost (Figs. 5E–J). In addition to the perturbation of the osteochondrogenic program, morphants showed a loss of *dlx2b* expression, suggesting that tooth development was also affected (Figs. 5K, L). Further examination of histological sections of 120 hpf *barx1* morphant larvae (n=2/5) showed condensation of tooth germs at an early cytodifferentiation stage of development whereas control larvae (n=3/3) exhibited erupted teeth (Supplementary Fig. S5). These data point to the importance of Barx1 function during the earliest stages of chondrogenesis.

Attenuation of barx1 enhances markers of jaw joint patterning

Morphants stained with Alcian Blue exhibited a range of altered cartilage morphology that included mispatterning of the joints (Figs. 3D–H). *Barx1* is expressed in the mouse and chick joints of the limbs and digits and has been suggested to regulate joint patterning by inhibiting chondrogenesis in limb micromass cultures (Tissier-Seta et al., 1995; Church et al., 2005). To determine the influence of *barx1* on joint patterning within the viscerocranium, we examined between 48 and 80 hpf molecular markers, *bapx1*, *chordin*, and *gdf5*, which are expressed in the developing jaw joint (Miller et al., 2003). Expression of *bapx1* at 48 hpf (Figs. 6A, B) and 56 hpf (data not shown), showed no to perhaps a mild enhancement in expression in morphant embryos. However, expression patterns of *chordin* as well as *gdf5* were noticeably enhanced within the jaw joint by the loss of *barx1* (open arrowheads, Figs. 6C–F). These results suggest that *barx1* influences the regulation of these two genes necessary for the proper patterning of the jaw joint in zebrafish.

barx1 is necessary for cellular proliferation of chondrogenic progenitors

We examined the effect of loss of *barx1* function on cell death and proliferation within the migrating neural crest streams and the pharyngeal arches. Control and *barx1* morphant embryos during migration and pharyngogenesis (13, 24 and 48 hpf) showed no apparent increase in apoptosis as determined by TUNEL labeling (data not shown). The hypoplastic arches suggested that *barx1* might participate in cellular proliferation. The pharyngeal arch mesenchyme was examined in serially sectioned control and *barx1* morphants stained with Phosphohistone-H3 (PH3) antibody at 34, 48, 56, and 72 hpf, a period of prominent arch outgrowth. Stained nuclei were counted within the arch ectomesenchyme, as indicated by the light green overlay marking the region of interest in Figs. 7A, B, in approximately 50 sections per embryo. The results show that *barx1* morphants exhibited 1.5 to 2.5-fold fewer dividing cells in the mesenchymal regions than control embryos at 48 and 56 hpf,

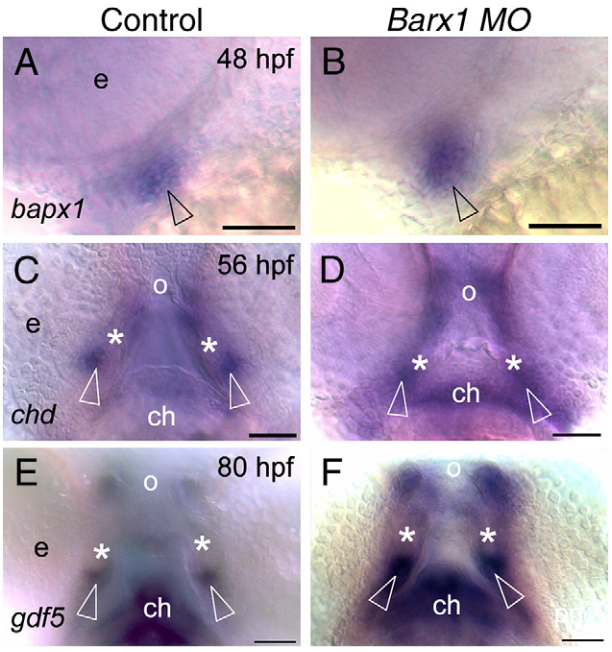

Fig. 6. Loss of *barx1* enhances *chordin* and *gdf5* expression in the jaw joint. Whole-mount *in situ* hybridization for (A, B) *bapx1*, (C, D) *chordin* (*chd*), and (E, F) *gdf5*. (A, C, E) Control uninjected embryos; (B, D, F) *barx1* morphants (see Fig. 4). Embryonic ages as indicated. (A, B) Lateral view, anterior to the left. (C–F) Ventral view, anterior at the top; asterisk indicates Meckel's cartilage, open arrowheads indicate jaw joint expression domains; e, eye; ch, ceratohyal; o orifice. Scale bar: (A–F) 50 μm.

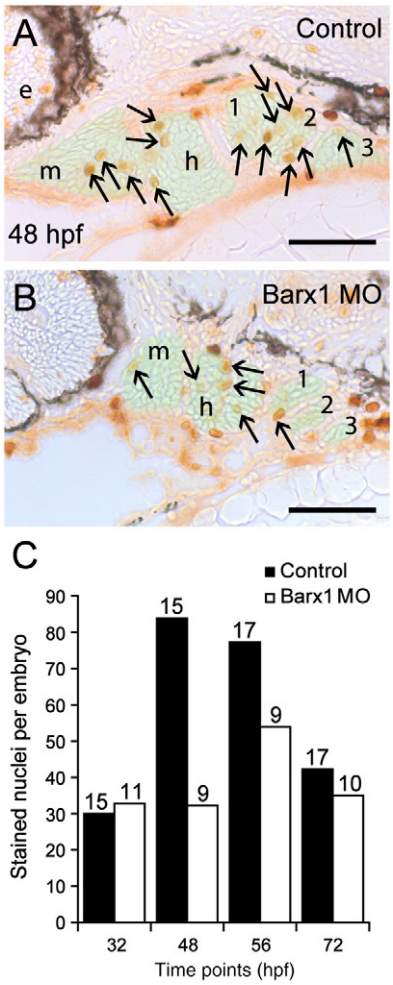

Fig. 7. *Barx1* positively influences cellular proliferation within the pharyngeal arches. (A, B) Sagittal serial sections (10 μm) of the pharyngeal arch region stained with Phosphohistone-H3 antibody. (A) Control embryo at 48 hpf. (B) *barx1* morphant. The neural crest derived mesenchyme is overlaid in green; arrows indicate stained nuclei; e, eye; m, mandibular arch; h, hyoid arch; gill arches are numbered. Anterior is to the left. Scale bar: 50 μm. (C) Averaged cell proliferation in control uninjected embryos (black bars) and *barx1* morphants (see Fig. 4; white bars) was determined within the mesenchyme as shown in panels A, B at the indicated four time points. Approximately fifty serial sections per embryo were examined. Number of embryos examined is indicated above each bar. Scale bar: (A, B) 50 μm.

but similar numbers at different time points (Fig. 7C). Since the decrease in PH3 labeled nuclei within the pharyngeal arch mesenchyme is at a critical period of arch outgrowth, our data suggest that *barx1* is involved in proliferation of the arch osteochondrogenic progenitors.

FGF signaling is necessary for barx1 expression in the pharyngeal arches

FGF signaling is required for proper pharyngeal arch patterning (Abu-Issa et al., 2002; David et al., 2002; Frank et al., 2002; Trokovic et al., 2003; Walshe and Mason, 2003; Crump et al., 2004; Trokovic et al., 2005). In chick and mouse, FGFs emanating from the oral ectoderm positively influence the underlying *Barx1* mesenchymal expression of the first arch (Tucker et al., 1998; Barlow et al., 1999). In zebrafish, *fgf8* and *fgf3* are expressed in the pharyngeal arch endoderm (Walshe and Mason, 2003). To determine the influence of FGF signaling on *barx1* expression in zebrafish, we examined the *fgf3* (*lia*) and the *fgf8* (*ace*) mutants. In *fgf3* mutants, larvae exhibit malformed mandibular and hyoid derived cartilages, and lack more posterior cartilages in the gill arches (Crump et al., 2004; Herzog et al., 2004). Expression of *barx1* was similarly affected in that transcripts were detected in the anterior arches but were reduced or lacking in the gill arches (arrows, Figs. 8A, B).

In *fgf8* mutants, left/right asymmetries were previously observed in pharyngeal arch cartilage patterning (Albertson and Yelick, 2005). Therefore, using *barx1* as a marker of chondrocyte condensation, we examined *ace* mutants for differences between control embryos and

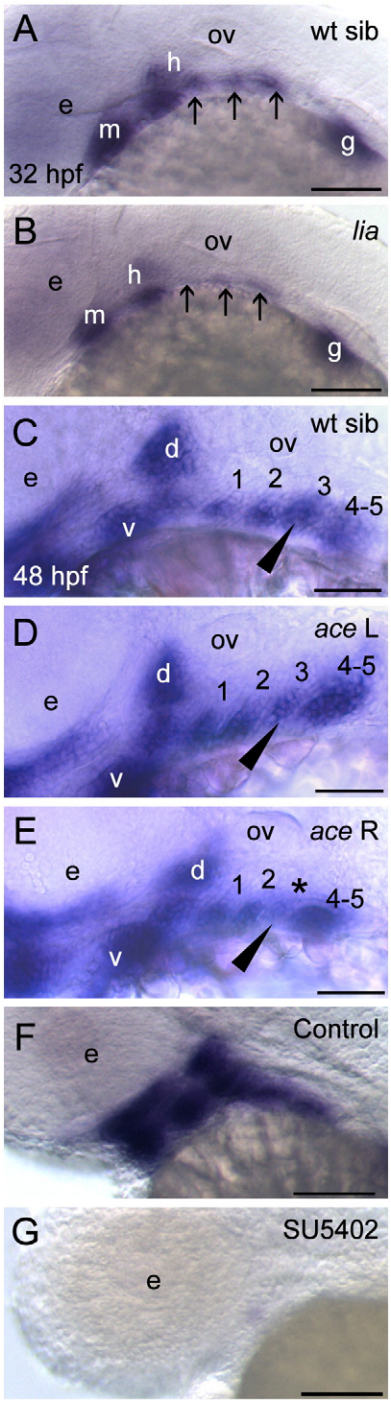

Fig. 8. *Barx1* expression in *fgf* mutant embryos. (A, B) Wild-type sibling and *lia/fgf3* mutant. Arrows indicate sites of *barx1* expression in the gill arches. (C–E) Wild-type sibling and left and right views of an *ace/fgf8* mutant embryo. Left/right asymmetric expression indicated in the mutant (arrowhead); asterisk indicates reduced expression in the third gill arch. (F, G) Overstained control (DMSO) and embryo treated with the FGF receptor inhibitor SU5402 from 24 hpf to 48 hpf. Lateral views with anterior to the left, panel D was flipped for comparison; d, dorsal and v, ventral expression domains of the second arch; e, eye; gill arches are numbered; g, gut primordium; h, hyoid arch; m, mandibular arch; ov, otic vesicle. Scale bar: (A–G) 50 μm.

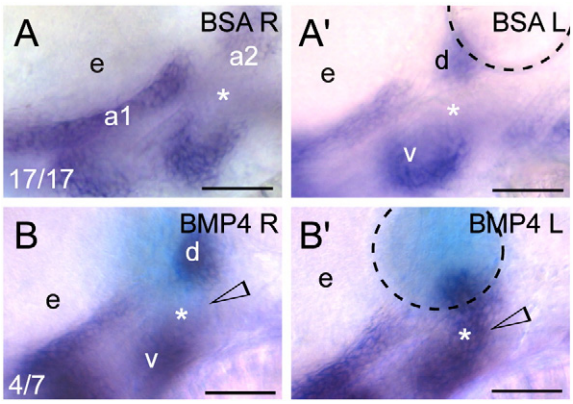

Fig. 9. Exogenous BMP signaling influences *barx1* expression within the zebrafish pharyngeal arches. (A, B) Whole-mount *in situ* hybridization of *barx1* in the left (bead implanted) and right (control) side of single embryos. Right-side images were flipped for easier comparison. (A, A′) Control BSA white bead, (B, B′) BMP4 blue bead. Anterior is to the left; d and v, dorsal and ventral expression domains in the second arch; e, eye. Arrowhead indicates sites of *barx1* misexpression; asterisk indicates intermediate region, normally devoid of *barx1* expression at this stage. Number of affected embryos over total embryos with successful bead implantation is indicated in the panels A, B. Black dashed line outlines the bead. Scale bar: 50 μm.

the left- and the right-hand sides of mutant embryos. Subtle differences were observed in the cellular condensation within the stacked arrays on the two sides of the same embryo in *ace* mutants (Figs. 8C–E); the differences included reduced (black arrowheads) or absence of *barx1* expression (asterisk). As multiple FGF ligands are expressed in the embryo, we blocked all FGF receptor signaling with the pharmacological inhibitor SU5402 (Mohammadi et al., 1997). Embryos soaked in the inhibitor beginning at 24 hpf and compared to control siblings at 48 hpf lose *barx1* expression (Figs. 8F, G). These data indicate that FGF signaling is necessary for maintaining *barx1* expression in the arches and suggests that several FGF ligands are involved in this process.

barx1 is influenced by exogenous BMP4 signaling within the hyoid arch intermediate zone

Signaling factors that include BMPs emanating from the encapsulating tissues are necessary for patterning the pharyngeal arches and influencing subsequent chondrogenesis (Hall and Miyake, 2000; Helms and Schneider, 2003; Goldring et al., 2006; Nie et al., 2006b). We examined the effects of exogenous BMP4 signaling on *barx1* expression. The effectiveness of using beads coated in BMPs has previously been demonstrated in chick and mouse organ cultures as well as in zebrafish embryos (Barlow and Francis-West, 1997; Tucker et al., 1998; Holzschuh et al., 2005). Beads were implanted on the left side at 24 hpf and the embryos were allowed to develop until 48 hpf. Control embryos were implanted with beads coated in 1% BSA (Figs. 9A, A′), and exhibited identical *barx1* expression on their left and right-hand sides (n=17/17). Embryos implanted with BMP4 coated beads expressed *barx1* within the intermediate domain of the second (hyoid) arch, where expression is not normally observed (open arrowhead in Figs. 9B, B′; n=4/7). Embryos implanted with BMP4 (n=11) beads at 36 hpf and examined at 60 hpf did not show any difference in *barx1* expression compared to the control side (data not shown). These observations indicate that BMP4 can lead to ectopic *barx1* expression within the hyoid intermediate zone with a regional and time-dependent specificity in the response.

Discussion

Endochondral bone formation is preceded by chondrogenesis that forms the anlage for shaping of the bones (Hall and Miyake, 2000; Karsenty and Wagner, 2002; Goldring et al., 2006). The viscerocranium consists of highly adapted skeletal elements necessary for mastication, auditory amplification, and vocalization (Sperber and Sperber, 1996). How these elements are patterned is not well understood. Here we report analysis of the zebrafish *barx1* transcription factor expression, its functional role in patterning chondrocyte condensation within the pharyngeal arches and the influence of morphogenic cues on its expression. Our experiments indicate that zebrafish *barx1* is essential for proper patterning of the osteochondrogenic progenitors within the pharyngeal arches.

Zebrafish barx1

We have characterized the zebrafish *barx1* gene and compared it to its paralogue, *barx2*. The expression of *barx1* in the zebrafish embryo shows both conserved and divergent patterns compared to the mouse and chick. In the mouse, *Barx1* is expressed in the mesenchyme of the maxillary facial prominences, restricted in the first and second arches to the lateral aspects abutting the stomodeum and the pharyngeal cavity, and is prominently found in the molar field, yet lacking in Meckel's cartilage condensations (Tissier-Seta et al., 1995). Expression is also observed in the mouse olfactory epithelium. In chick, *Barx1* is expressed in the mesenchyme and the epithelium of the facial primordia and is detected after neural crest migration into the arches (Barlow et al., 1999). *Barx* genes further are expressed in articular cartilage and the epiphyseal growth plate (Tissier-Seta et al., 1995; Barlow et al., 1999; Church et al., 2005; Meech et al., 2005). In contrast, zebrafish *barx1* expression is detected early in the migrating hindbrain-derived neural crest and subsequently throughout the pharyngeal arch mesenchyme. As chondrogenesis progresses, *barx1* expression is downregulated in arrayed cells (Fig. 2I) while being maintained in the surrounding mesenchyme, suggesting that loss of *barx1* expression may be a prerequisite for osteogenic differentiation. *Barx1* expression was not detected in the ethmoid plate or trabeculae of the neurocranium, even though midbrain–hindbrain neural crest contributes to these structures, which undergo endochondral bone formation (Eberhart et al., 2006). These observations illustrate genetic differences in the chondrogenic program of neural crest cells derived from a similar location undergoing condensation within different elements of the chondrocranium. In comparison, *barx2* is expressed most prominently in the oral and aboral epithelium of the first and second arches as well as in the olfactory epithelium, but not in the gut, and is therefore divergent of the observed pattern in higher vertebrates (Tissier-Seta et al., 1995; Barlow et al., 1999; Sander and Powell, 2004). Comparison of these patterns suggests that an alternate evolutionary subfunctionalization of the *barx* genes has occurred in teleosts in contrast to higher vertebrate model systems. *Barx1* expression was also conserved in the developing gut wall in zebrafish as in the mouse and chick, as well as in the pectoral fin/limb buds. Transient expression was detected in the posterior lateral line ganglia at 72 hpf. Additional transient expression from 24 to 32 hpf was observed in the somite chevrons of the trunk and tail.

Initial arch patterning is maintained in barx1 morphants

The loss of *barx1* function does not affect the specification of the cranial neural crest or the initial patterning of the pharyngeal arches as expression of neural crest markers *dlx2a* and *inca* is maintained during migration in *barx1* morphants. Initial arch patterning appears normal as the pouches form when visualized in the *fli1:GFP* transgenic line. The behavior of other derivatives of the neural crest, such as aspects of the facial ganglia, which express *neuroD* and melanophores responsible for pigment, indicate that their respective differentiation is maintained in the morphants. As development progresses, however, we observed dysmorphogenesis within the pouches, presumably because of reduced cellular proliferation and compromised cellular condensation.

Chondrocyte differentiation requires barx1 in the pharyngeal arches

Two phases have been recognized in cartilage morphogenesis of the zebrafish pharyngeal arches, deposition of matrix by condensed chondrocytes, and a period of rapid growth (Kimmel et al., 1998). *Barx* genes regulate the cell adhesion molecule NCAM (Hirsch et al., 1991; Edelman et al., 2000), which is expressed in aggregating prechondrocytes (Widelitz et al., 1993; DeLise et al., 2000; Hall and Miyake, 2000), and the fibril-forming type II collagen (*Col2a1*), the main component of cartilage extracellular matrix (Meech et al., 2005). Here we show that attenuation of *barx1* resulted in poor facial outgrowth due to fewer chondrocytes and poor deposition of matrix, causing dysmorphic cartilage elements as shown by poor fusion between the symplectic and hyomandibular elements (Fig. 3H). We observed that *barx1* morphants cause the perturbation of osteogenic promoting factors that include *runx2b* and *chondromodulin* (Fig. 5). Additionally, factors co-expressed in the arch neural crest, *dlx2a* and *sox9a*, which are required for chondrogenesis maintain their expression in the *barx1* morphants. These observations suggest that *barx1* functions at the earliest stages of prechondrocyte aggregation in an apparently independent regulatory mechanism compared to other cartilage and bone associated transcription factors. We further observed an enhancement in *chordin* and *gdf5* expression within the jaw joint of morphants. Meech et al. (2005) showed that Gdf5 is able to induce *Barx2* expression, suggesting a functional connection. Here we show that the loss of the *barx1* induces *gdf5* expression, suggesting a potential negative feedback regulatory mechanism that may function to balance their respective roles in chondrogenesis and joint patterning.

FGF and BMP signaling influence barx1 expression in the pharyngeal arches

Reciprocal epithelial–mesenchymal interactions mediated by BMPs are essential for pharyngeal arch patterning and chondrogenesis (Tucker et al., 1998; Barlow et al., 1999; Tucker et al., 1999; Mina et al., 2002; Nie et al., 2006b). During chondrogenesis, FGF and BMP signaling is thought to act antagonistically, balancing proliferation and terminal differentiation in a complex regulatory network (Minina et al., 2002; Ornitz, 2005; Nie et al., 2006a; Nie et al., 2006b). In higher vertebrates, FGF8 and BMP2/4 induce and negatively influence *Barx1* expression, respectively, in the maxillary and mandibular prominences (Tucker et al., 1998; Barlow et al., 1999). Conversely, in limb cultures, BMP4 positively influences *Barx2* expression (Meech et al., 2005). Fgf8 and Fgf3 emanating from the endoderm, participate in the segmentation of the arches in zebrafish by promoting neural crest survival and cellular proliferation (Walshe and Mason, 2003; Crump et al., 2004). In our report, *fgf3* and *fgf8* deficient fish perturb but do not abolish *barx1* expression. However, incubation with SU5402, a FGF receptor antagonist, completely abolishes *barx1* expression. These data suggest that multiple FGFs are necessary to regulate and maintain *barx1* expression in an apparent coordinate manner.

BMP signaling is involved at different stages of the chondrogenic program (Yoon and Lyons, 2004), and BMPs emanate from the pouch endoderm of the zebrafish arches (Holzschuh et al., 2005). BMP2/4 beads implanted in the chick mandible show loss of surrounding *Barx1* expression (Tucker et al., 1998; Barlow et al., 1999). However, we observed that BMP4 bead implantation induced ectopic *barx1* expression within the receptive cells of the second arch intermediate region. Taken together, these reports and our data suggest that *barx1* expression influenced by BMP cues reflect the cellular proliferation and extracellular matrix production necessary for shaping of cartilage elements within the viscerocranium.

Acknowledgments

We thank Pfizer Inc. for the generous gift of the SU5402, Dr. Chisa Shukunami for *chondromodulin*, Dr. Matthias Hammerschmidt for the *lia* embryos; Drs. Tom Sargent and Ting Luo for the *inca* probe, Dr. Marc Ekker for the *dlx2b* probe, our laboratory colleagues for their helpful discussions, Dr. G.H. Sperber and the NIH Fellows Editorial Board for their comments on the manuscript, and Mark Rath and John Gonzales for their assistance with zebrafish husbandry. This research has been supported by the Intramural Program of the NICHD, NIH.

Appendix A. Supplementary data

Supplementary data associated with this article can be found, in the online version, at doi:10.1016/j.ydbio.2008.06.004.

References

Abu-Issa, R., Smyth, G., Smoak, I., Yamamura, K.-i., Meyers, E.N., 2002. Fgf8 is required for pharyngeal arch and cardiovascular development in the mouse. Development 129, 4613–4625.
Akimenko, M.A., Ekker, M., Wegner, J., Lin, W., Westerfield, M., 1994. Combinatorial expression of three zebrafish genes related to distal-less: part of a homeobox gene code for the head. J. Neurosci. 14, 3475–3486.
Albertson, R.C., Yelick, P.C., 2005. Roles for fgf8 signaling in left–right patterning of the visceral organs and craniofacial skeleton. Dev. Biol. 283, 310–321.
Angelo, S., Lohr, J., Lee, K.H., Ticho, B.S., Breitbart, R.E., Hill, S., Yost, H.J., Srivastava, D., 2000. Conservation of sequence and expression of *Xenopus* and zebrafish dHAND during cardiac, branchial arch and lateral mesoderm development. Mech. Dev. 95, 231–237.
Barlow, A.J., Bogardi, J.P., Ladher, R., Francis-West, P.H., 1999. Expression of chick Barx-1 and its differential regulation by FGF-8 and BMP signaling in the maxillary primordia. Dev. Dyn. 214, 291–302.
Barlow, A.J., Francis-West, P.H., 1997. Ectopic application of recombinant BMP-2 and BMP-4 can change patterning of developing chick facial primordia. Development 124, 391–398.
Chiang, E.F., Pai, C.I., Wyatt, M., Yan, Y.L., Postlethwait, J., Chung, B., 2001. Two sox9 genes on duplicated zebrafish chromosomes: expression of similar transcription activators in distinct sites. Dev. Biol. 231, 149–163.
Church, V., Yamaguchi, K., Tsang, P., Akita, K., Logan, C., Francis-West, P., 2005. Expression and function of Bapx1 during chick limb development. Anat. Embryol. (Berl). 209, 461–469.
Crump, J.G., Maves, L., Lawson, N.D., Weinstein, B.M., Kimmel, C.B., 2004. An essential role for Fgfs in endodermal pouch formation influences later craniofacial skeletal patterning. Development 131, 5703–5716.
David, N.B., Saint-Etienne, L., Tsang, M., Schilling, T.F., Rosa, F.M., 2002. Requirement for endoderm and FGF3 in ventral head skeleton formation. Development 129, 4457–4468.
de Crombrugghe, B., Lefebvre, V., Behringer, R.R., Bi, W., Murakami, S., Huang, W., 2000. Transcriptional mechanisms of chondrocyte differentiation. Matrix Biol. 19, 389–394.
DeLise, A.M., Fischer, L., Tuan, R.S., 2000. Cellular interactions and signaling in cartilage development. Osteoarthr. Cartil. 8, 309–334.
Eberhart, J.K., Swartz, M.E., Crump, J.G., Kimmel, C.B., 2006. Early Hedgehog signaling from neural to oral epithelium organizes anterior craniofacial development. Development 133, 1069–1077.
Edelman, D.B., Meech, R., Jones, F.S., 2000. The homeodomain protein Barx2 contains activator and repressor domains and interacts with members of the CREB family. J. Biol. Chem. 275, 21737–21745.
Ellies, D.L., Langille, R.M., Martin, C.C., Akimenko, M.A., Ekker, M., 1997. Specific craniofacial cartilage dysmorphogenesis coincides with a loss of dlx gene expression in retinoic acid-treated zebrafish embryos. Mech. Dev. 61, 23–36.
Flores, M.V., Lam, E.Y., Crosier, P., Crosier, K., 2006. A hierarchy of Runx transcription factors modulate the onset of chondrogenesis in craniofacial endochondral bones in zebrafish. Dev. Dyn. 235, 3166–3176.
Flores, M.V., Tsang, V.W., Hu, W., Kalev-Zylinska, M., Postlethwait, J., Crosier, P., Crosier, K., Fisher, S., 2004. Duplicate zebrafish runx2 orthologues are expressed in developing skeletal elements. Gene Expr. Patterns 4, 573–581.
Frank, D.U., Fotheringham, L.K., Brewer, J.A., Muglia, L.J., Tristani-Firouzi, M., Capecchi, M.R., Moon, A.M., 2002. An Fgf8 mouse mutant phenocopies human 22q11 deletion syndrome. Development 129, 4591–4603.
Goldring, M.B., Tsuchimochi, K., Ijiri, K., 2006. The control of chondrogenesis. J. Cell Biochem. 97, 33–44.
Gould, D.B., Walter, M.A., 2000. Cloning, characterization, localization, and mutational screening of the human BARX1 gene. Genomics 68, 336–342.
Gould, D.B., Walter, M.A., 2004. Mutational analysis of BARHL1 and BARX1 in three new patients with Joubert syndrome. Am. J. Med. Genet. A. 131, 205–208.
Hall, B.K., Miyake, T., 2000. All for one and one for all: condensations and the initiation of skeletal development. BioEssays 22, 138–147.
Helms, J.A., Schneider, R.A., 2003. Cranial skeletal biology. Nature 423, 326–331.
Herzog, W., Sonntag, C., von der Hardt, S., Roehl, H.H., Varga, Z.M., Hammerschmidt, M., 2004. Fgf3 signaling from the ventral diencephalon is required for early specification and subsequent survival of the zebrafish adenohypophysis. Development 131, 3681–3692.
Hirsch, M., Valarche, I., Deagostini-Bazin, H., Pernelle, C., Joliot, A., Goridis, C., 1991. An upstream regulatory element of the NCAM promoter contains a binding site for homeodomains. FEBS Lett. 287, 197–202.

Hjalt, T.A., Murray, J.C., 1999. The human BARX2 gene: genomic structure, chromosomal localization, and single nucleotide polymorphisms. Genomics 62, 456–459.
Holzschuh, J., Wada, N., Wada, C., Schaffer, A., Javidan, Y., Tallafuss, A., Bally-Cuif, L., Schilling, T.F., 2005. Requirements for endoderm and BMP signaling in sensory neurogenesis in zebrafish. Development 132, 3731–3742.
Jackman, W.R., Draper, B.W., Stock, D.W., 2004. Fgf signaling is required for zebrafish tooth development. Dev. Biol. 274, 139–157.
Jones, F.S., Kioussi, C., Copertino, D.W., Kallunki, P., Holst, B.D., Edelman, G.M., 1997. Barx2, a new homeobox gene of the Bar class, is expressed in neural and craniofacial structures during development. Proc. Natl. Acad. Sci. U. S. A. 94, 2632–2637.
Karsenty, G., Wagner, E.F., 2002. Reaching a genetic and molecular understanding of skeletal development. Dev. Cell 2, 389–406.
Kim, B.-M., Buchner, G., Miletch, I., Sharpe, P.T., Shivdasani, R.A., 2005. The stomach mesenchymal transcription factor Barx1 specifies gastric epithelial identity through inhibition of transient Wnt signaling. Dev. Cell 8, 611–622.
Kimmel, C.B., Miller, C.T., Kruze, G., Ullmann, B., BreMiller, R.A., Larison, K.D., Snyder, H.C., 1998. The shaping of pharyngeal cartilages during early development of the zebrafish. Dev. Biol. 203, 245–263.
Korzh, V., Sleptsova, I., Liao, J., He, J., Gong, Z., 1998. Expression of zebrafish bHLH genes ngn1 and nrd defines distinct stages of neural differentiation. Dev. Dyn. 213, 92–104.
Lawson, N.D., Weinstein, B.M., 2002. In vivo imaging of embryonic vascular development using transgenic zebrafish. Dev. Biol. 248, 307–318.
Luo, R., An, M., Arduini, B.L., Henion, P.D., 2001. Specific pan-neural crest expression of zebrafish Crestin throughout embryonic development. Dev. Dyn. 220, 169–174.
Luo, T., Xu, Y., Hoffman, T.L., Zhang, T., Schilling, T., Sargent, T.D., 2007. Inca: a novel p21-activated kinase-associated protein required for cranial neural crest development. Development 134, 1279–1289.
Meech, R., Edelman, D.B., Jones, F.S., Makarenkova, H.P., 2005. The homeobox transcription factor Barx2 regulates chondrogenesis during limb development. Development 132, 2135–2146.
Miletich, I., Buchner, G., Sharpe, P.T., 2005. Barx1 and evolutionary changes in feeding. J. Anat. 207, 619–622.
Miller, C.T., Yelon, D., Stainier, D.Y., Kimmel, C.B., 2003. Two endothelin 1 effectors, hand2 and bapx1, pattern ventral pharyngeal cartilage and the jaw joint. Development 130, 1353–1365.
Mina, M., Wang, Y.H., Ivanisevic, A.M., Upholt, W.B., Rodgers, B., 2002. Region- and stage-specific effects of FGFs and BMPs in chick mandibular morphogenesis. Dev. Dyn. 223, 333–352.
Minina, E., Kreschel, C., Naski, M.C., Ornitz, D.M., Vortkamp, A., 2002. Interaction of FGF, Ihh/Pthlh, and BMP signaling integrates chondrocyte proliferation and hypertrophic differentiation. Dev. Cell 3, 439–449.
Mitsiadis, T.A., Drouin, J., 2008. Deletion of the Pitx1 genomic locus affects mandibular tooth morphogenesis and expression of the Barx1 and Tbx1 genes. Dev. Biol. 313, 887–896.
Mohammadi, M., McMahon, G., Sun, L., Tang, C., Hirth, P., Yeh, B.K., Hubbard, S.R., Schlessinger, J., 1997. Structures of the tyrosine kinase domain of fibroblast growth factor receptor in complex with inhibitors. Science 276, 955–960.
Motoike, T., Loughna, S., Perens, E., Roman, B.L., Liao, W., Chau, T.C., Richardson, C.D., Kawate, T., Kuno, J., Weinstein, B.M., Stainier, D.Y., Sato, T.N., 2000. Universal GFP reporter for the study of vascular development. Genesis 28, 75–81.
Nie, X., Luukko, K., Kettunen, P., 2006a. FGF signalling in craniofacial development and developmental disorders. Oral Dis. 12, 102–111.
Nie, X., Luukko, K., Kettunen, P., 2006b. BMP signalling in craniofacial development. Int. J. Dev. Biol. 50, 511–521.
Ornitz, D.M., 2005. FGF signaling in the developing endochondral skeleton. Cytokine Growth Factor Rev. 16, 205–213.
Redon, R., Baujat, G., Sanlaville, D., Le Merrer, M., Vekemans, M., Munnich, A., Carter, N.P., Cormier-Daire, V., Colleaux, L., 2006. Interstitial 9q22.3 microdeletion: clinical and molecular characterisation of a newly recognised overgrowth syndrome. Eur. J. Hum. Genet. 14, 759–767.
Rubinstein, A.L., Lee, D., Luo, R., Henion, P.D., Halpern, M.E., 2000. Genes dependent on zebrafish cyclops function identified by AFLP differential gene expression screen. Genesis 26, 86–97.
Sachdev, S.W., Dietz, U.H., Oshima, Y., Lang, M.R., Knapik, E.W., Hiraki, Y., Shukunami, C., 2001. Sequence analysis of zebrafish chondromodulin-1 and expression profile in the notochord and chondrogenic regions during cartilage morphogenesis. Mech. Dev. 105, 157–162.
Sander, G.R., Powell, B.C., 2004. Expression of the homeobox gene barx2 in the gut. J. Histochem. Cytochem. 52, 541–544.
Schulte-Merker, S., Hammerschmidt, M., Beuchle, D., Cho, K.W., De Robertis, E.M., Nüsslein-Volhard, C., 1994. Expression of zebrafish *goosecoid* and *no tail* gene products in wild-type and mutant *no tail* embryos. Development 120, 843–852.
Song, Y., Zhang, Z., Yu, X., Yan, M., Zhang, X., Gu, S., Stuart, T., Liu, C., Reiser, J., Zhang, Y., Chen, Y., 2006. Application of lentivirus-mediated RNAi in studying gene function in mammalian tooth development. Dev. Dyn. 235, 1347–1357.
Sperber, G.H., Sperber, S.M., 1996. Pharyngogenesis. J. Dent. Assoc. S. Afr. 51, 777–782.
Stachel, S.E., Grunwald, D.J., Myers, P.Z., 1993. Lithium perturbation and goosecoid expression identify a dorsal specification pathway in the pregastrula zebrafish. Development 117, 1261–1274.
Stalker, H., Ayme, S., Delneste, D., Scarpelli, H., Vekemans, M., Der Kaloustian, V.M., 1993. Duplication of 9q12–q33: a case report and implications for the dup(9q) syndrome. Am. J. Med. Genet. 45, 456–459.
Tissier-Seta, J.P., Mucchielli, M.L., Mark, M., Mattei, M.G., Goridis, C., Brunet, J.F., 1995. Barx1, a new mouse homeodomain transcription factor expressed in cranio-facial ectomesenchyme and the stomach. Mech. Dev. 51, 3–15.
Trokovic, N., Trokovic, R., Mai, P., Partanen, J., 2003. Fgfr1 regulates patterning of the pharyngeal region. Genes Dev. 17, 141–153.
Trokovic, N., Trokovic, R., Partanen, J., 2005. Fibroblast growth factor signalling and regional specification of the pharyngeal ectoderm. Int. J. Dev. Biol. 49, 797–805.
Tuan, R.S., 2004. Biology of developmental and regenerative skeletogenesis. Clin. Orthop. Relat. Res. S105–117.
Tucker, A.S., Matthews, K.L., Sharpe, P.T., 1998. Transformation of tooth type induced by inhibition of BMP signaling. Science 282, 1136–1138.
Tucker, A.S., Yamada, G., Grigoriou, M., Pachnis, V., Sharpe, P.T., 1999. Fgf-8 determines rostral–caudal polarity in the first branchial arch. Development 126, 51–61.
Walker, M.B., Miller, C.T., Coffin Talbot, J., Stock, D.W., Kimmel, C.B., 2006. Zebrafish *furin* mutants reveal intricacies in regulating Endothelin1 signaling in craniofacial patterning. Dev. Biol. 295, 194–205.
Walker, M.B., Miller, C.T., Swartz, M.E., Eberhart, J.K., Kimmel, C.B., 2007. *phospholipase C, beta 3* is required for Endothelin1 regulation of pharyngeal arch patterning in zebrafish. Dev. Biol. 304, 194–207.
Walshe, J., Mason, I., 2003. Fgf signalling is required for formation of cartilage in the head. Dev. Biol. 264, 522–536.
Westerfield, M., 1995. The Zebrafish Book. University of Oregon Press, Eugene.
Widelitz, R., Jiang, T., Murray, B., Chuong, C., 1993. Adhesion molecules in skeletogenesis: II. Neural cell adhesion molecules mediate precartilaginous mesenchymal condensations and enhance chondrogenesis. J. Cell. Physiol. 156, 399–411.
Yan, Y.L., Hatta, K., Riggleman, B., Postlethwait, J.H., 1995. Expression of a type II collagen gene in the zebrafish embryonic axis. Dev. Dyn. 203, 363–376.
Yan, Y.L., Miller, C.T., Nissen, R.M., Singer, A., Liu, D., Kirn, A., Draper, B., Willoughby, J., Morcos, P.A., Amsterdam, A., Chung, B.C., Westerfield, M., Haffter, P., Hopkins, N., Kimmel, C., Postlethwait, J.H., Nissen, R., 2002. A zebrafish sox9 gene required for cartilage morphogenesis. Development 129, 5065–5079.
Yan, Y.L., Willoughby, J., Liu, D., Crump, J.G., Wilson, C., Miller, C.T., Singer, A., Kimmel, C., Westerfield, M., Postlethwait, J.H., 2005. A pair of Sox: distinct and overlapping functions of zebrafish sox9 co-orthologs in craniofacial and pectoral fin development. Development 132, 1069–1083.
Yoon, B.S., Lyons, K.M., 2004. Multiple functions of BMPs in chondrogenesis. J. Cell. Biochem. 93, 93–103.